Journal of Alloys and Compounds 595 (2014) 28–32

Contents lists available at ScienceDirect

Journal of Alloys and Compounds

journal homepage: www.elsevier.com/locate/jalcom

Hydrogen dynamics in Laves-phase hydride $YFe_2H_{2.6}$: Inelastic and quasielastic neutron scattering studies

A.V. Skripov [a,*], V. Paul-Boncour [b], T.J. Udovic [c], J.J. Rush [a,d]

[a] Institute of Metal Physics, Ural Branch of the Russian Academy of Sciences, Ekaterinburg 620990, Russia
[b] Institute of Chemistry and Materials of Paris East, CMTR, CNRS and UPAC, 94320 Thiais Cedex, France
[c] NIST Center for Neutron Research, National Institute of Standards and Technology, Gaithersburg, Maryland 20899-6102, USA
[d] Department of Materials Science and Engineering, University of Maryland, College Park, Maryland 20742-2115, USA

ARTICLE INFO

Article history:
Received 16 December 2013
Received in revised form 20 January 2014
Accepted 20 January 2014
Available online 28 January 2014

Keywords:
Metal hydrides
Diffusion
Inelastic neutron scattering

ABSTRACT

The vibrational spectrum of hydrogen and the parameters of H jump motion in the C15-type compound $YFe_2H_{2.6}$ have been studied by means of inelastic and quasielastic neutron scattering. It is found that hydrogen atoms occupying tetrahedral interstitial *g* (Y_2Fe_2) sites participate in the fast localized jump motion. The behavior of the elastic incoherent structure factor as a function of momentum transfer (measured up to $Q_{max} \approx 4$ Å^{-1}) is consistent with the two-site motion of H atoms within pairs of closely spaced *g* sites. In the studied *T* range of 140–390 K, the temperature dependence of the jump rate of this localized motion is found to be non-Arrhenius; however, it can be described by two Arrhenius-like terms with the activation energies of 42 and 10 meV in the ranges 295–390 K and 140–240 K, respectively. Our results also indicate that hydrogen dynamics in $YFe_2H_{2.6}$ is affected by considerable local lattice distortions resulting from hydrogenation of YFe_2.

1. Introduction

Laves phase intermetallics composed of yttrium (or rare-earth element) and a transition metal can absorb large amounts of hydrogen forming hydrides with interesting physical properties [1]. Among these compounds, the YFe_2–H(D) system is of particular interest due to the rich variety of crystal structures derived from the cubic C15-type structure of the parent intermetallic at different hydrogen concentrations [2]. Seven different crystal structures have been reported for this system, starting from the tetragonal structure for $YFe_2D_{1.2}$ to the orthorhombic structure for the deuterium-rich YFe_2D_5 [3,4]. Such a complex phase diagram is expected to originate from the ordering of H(D) atoms that can be accompanied by lattice distortions and/or superstructures below the ordering temperature. The processes of hydrogen redistribution among the available interstitial sites require certain mobility of H atoms. However, the dynamical properties of hydrogen in YFe_2 have not been investigated so far. In the present work, we use inelastic and quasielastic neutron scattering to study H dynamics in the hydride $YFe_2H_{2.6}$ retaining the cubic C15-type host-metal structure of the YFe_2 intermetallic.

One of the most unusual features of hydrogen diffusion in Laves phase compounds is the coexistence of two types of H jumps with different characteristic rates. It has been found [5,6] that in those C15-type Laves phases AB_2 where hydrogen atoms occupy only tetrahedral interstitial *g* sites (with A_2B_2 coordination), the faster jump process corresponds to the localized H motion within the regular hexagons formed by *g* sites, and the slower process is associated with H jumps from one *g*-site hexagon to another. The difference between the characteristic rates of these jumps is expected to originate from the difference between the nearest-neighbor *g*–*g* distances r_1 (within the hexagons) and r_2 (between the nearest hexagons), see Fig. 1. The value of r_2/r_1 is determined by the positional parameters of H atoms at *g* sites; these parameters are found to depend strongly on the ratio of the metallic radii R_A and R_B of the elements *A* and *B* [6]. The localized H motion has been investigated mostly in C15-type compounds with $R_A/R_B \leqslant 1.25$ where $r_2/r_1 > 1$ (changing from 1.07 for $ZrCr_2H_x$ to 1.45 for TaV_2H_x [6]). For compounds with $R_A/R_B > 1.3$, the *g*–*g* distance r_2 is expected to become shorter than r_1. This may give rise to a qualitative change in the microscopic picture of H motion: the faster jump process should be transformed into the back-and-forth jumps within *pairs* of *g* sites separated by r_2. The only C15-type system where such a two-site localized motion has been observed experimentally [7,8] is YMn_2H_x with $r_2/r_1 = 0.82$. The results of the neutron diffraction study [2] of $YFe_2D_{2.6}$ at room temperature have

* Corresponding author. Tel.: +7 343 378 3781; fax: +7 343 374 5244.
E-mail address: skripov@imp.uran.ru (A.V. Skripov).

http://dx.doi.org/10.1016/j.jallcom.2014.01.154
0925-8388/

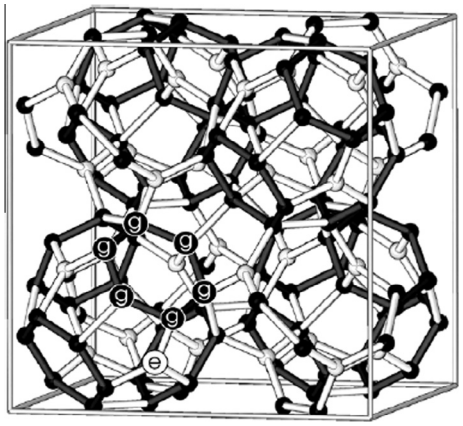

Fig. 1. The spatial arrangement of interstitial *g* sites (dark spheres) and *e* sites (light spheres) in the cubic C15-type AB_2 compound. Each *g* site has three *g*-site neighbors: two *g* sites on the same hexagon at a distance of r_1 (dark bars) and one *g* site on the adjacent hexagon at a distance of r_2 (light bars). Metal atoms are not shown. Each *g* site is coordinated by 2 *A* and 2 *B* atoms, and each *e* site is coordinated by 1 *A* and 3 *B* atoms.

shown that D atoms in this compound randomly occupy *g* sites with the positional parameters $x_g = 0.339$, $z_g = 0.141$. Using these structural data for $YFe_2D_{2.6}$, we find that $r_2 = 0.79$ Å, $r_1 = 1.50$ Å, and $r_2/r_1 = 0.53$. It should be noted that the value of r_2 for $YFe_2D_{2.6}$ is the shortest *g*–*g* distance ever found for hydrogen-absorbing Laves phases. Thus, the YFe_2–H(D) system offers a good opportunity to verify the relation between r_2/r_1 and the microscopic picture of localized H motion in cubic Laves phase compounds. In the present work, quasielastic neutron scattering (QENS) is applied to study the mechanism and parameters of hydrogen jump motion in $YFe_2H_{2.6}$ over a wide temperature range. QENS experiments are complemented by an inelastic neutron scattering (INS) measurement of the hydrogen vibrational spectrum, which is sensitive to the local environment of H atoms in $YFe_2H_{2.6}$.

2. Experimental details

The sample preparation was analogous to that described in Refs. [9] and [10]. The intermetallic compound YFe_2 was prepared by induction melting of pure Y (99.9%) and Fe (99.99%) followed by annealing in vacuum for 12 days at 1163 K. The composition and homogeneity of the intermetallic compound were checked by electron probe microanalysis and X-ray diffraction. According to X-ray diffraction analysis, the resulting YFe_2 sample was a single-phase compound with the cubic C15-type structure (space group $Fd\bar{3}m$) and the lattice parameter $a = 7.362$ Å. Before hydrogen absorption, the powdered sample was activated by heat treatment at 363 K in vacuum. The hydride was prepared by solid–gas reaction at 408 K using a Sieverts-type apparatus. In order to avoid sample amorphisation or decomposition, the rate of H_2 admission was kept low. The hydrogen content was measured by recording the pressure variation in calibrated and thermostated volumes. According to X-ray diffraction, the resulting $YFe_2H_{2.6}$ hydride retained the single-phase state with the same C15-type host-metal lattice, but with larger lattice parameter ($a = 7.782$ Å). This value of *a* is in good agreement with previous data [2] for the same composition.

All neutron scattering experiments were performed at the NIST Center for Neutron Research (Gaithersburg, Maryland, USA). The inelastic neutron scattering measurement of the hydrogen vibrational spectrum at 4 K was made on a filter-analyzer neutron spectrometer (FANS) [11] using the Cu(2 2 0) monochromator and horizontal collimation of 20 min of arc before and after the monochromator. The measured range of neutron energy loss was 50–210 meV, and the energy resolution was about 4–5% of the energy transfer. Measurements of QENS spectra $S_{exp}(Q, \omega)$ (where $\hbar\omega$ is the energy transfer and $\hbar Q$ is the elastic momentum transfer) were performed on the time-of-flight disk-chopper spectrometer (DCS) [12] using the incident neutron wavelengths λ of 5.0 Å and 2.75 Å. The energy resolution full widths at half-maximum (FWHM) were 105 μeV ($\lambda = 5.0$ Å) and 270 μeV ($\lambda = 2.75$ Å). The ranges of the elastic momentum transfer studied corresponded to *Q* ranges of 0.63–2.01 $Å^{-1}$ ($\lambda = 5.0$ Å) and 1.17–3.94 $Å^{-1}$ ($\lambda = 2.75$ Å). The powdered $YFe_2H_{2.6}$ sample was studied in annular geometry in a hollow-cylinder Al container, the sample thickness being ~0.3 mm. The sample thickness was chosen to ensure ~90% neutron transmission and thus minimize multiple-scattering effects. QENS spectra were recorded at $T = 30$, 140, 170, 200, 240, 270, 295, 330, 360 and 390 K with $\lambda = 5.0$ Å, and at $T = 30$, 240 and 360 K with $\lambda = 2.75$ Å. For analysis of the DCS data, the detectors were binned into eight or nine groups. The scattering angles corresponding to the Bragg reflections were excluded from the analysis. The instrumental resolution functions $R(Q, \omega)$ were determined from the measured QENS spectra for $YFe_2H_{2.6}$ at low temperature (30 K).

3. Results and discussion

3.1. Neutron vibrational spectroscopy

The experimental low-temperature INS spectrum for $YFe_2H_{2.6}$ is shown in Fig. 2. It consists of two broad peaks centered at ~97 and ~150 meV with a nearly 1:2 intensity ratio. The simplest approach to the description of INS spectra due to localized hydrogen vibrations is based on the model of a three-dimensional Einstein oscillator [13,14]. For the $\hbar\omega$ range of fundamental modes, this model predicts three peaks of nearly equal intensity. Depending on point symmetry of H sites, all or two of these peaks may be degenerate. For hydrogen at *g* sites of the C15-type lattice, we expect three non-degenerate peaks, since the point symmetry (*m*) of these sites is lower than axial. General features of the experimental INS spectrum for $YFe_2H_{2.6}$ can be ascribed to H atoms at *g* sites (two unresolved peaks in the range 125–170 meV and a third peak in the range 82–117 meV). Comparing the shape of INS spectrum for $YFe_2H_{2.6}$ with those for other Laves-phase hydrides with partially occupied *g* sites [15–18], we can conclude that $YFe_2H_{2.6}$ exhibits the largest width of the main two peaks. While the broadening of the spectral features can be usually attributed to the dispersion of the corresponding bands due to H–H interactions, the large width of the peaks for $YFe_2H_{2.6}$ also suggests that the host-metal lattice in this compound is locally distorted, although it retains the average C15-type structure. This is consistent with the results of extended X-ray absorption fine structure (EXAFS) studies [19] for C15-type YFe_2D_x ($x = 2.5$ and 2.9) showing the presence of considerable distributions of Fe–Fe distances in these deuterides.

3.2. Quasielastic neutron scattering

Since the incoherent scattering cross-section of hydrogen is very large, the observed neutron scattering from our $YFe_2H_{2.6}$ sample is dominated by the incoherent nuclear scattering on protons. We have found that at $T \geqslant 140$ K the measured QENS spectra are satisfactorily described by a sum of two components: an 'elastic' line represented by the spectrometer resolution function and a resolution-broadened Lorentzian 'quasielastic' line. The relative intensity of the 'quasielastic' component increases with increasing

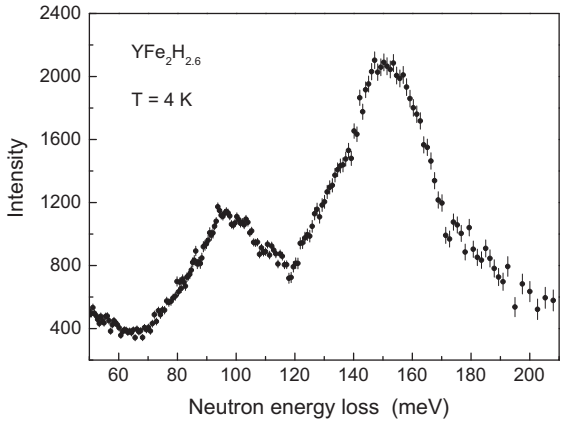

Fig. 2. The low-temperature inelastic neutron scattering spectrum for $YFe_2H_{2.6}$. Vertical error bars correspond to one standard deviation.

Q, its half-width being nearly Q-independent. These features are typical of the case of spatially-restricted (localized) atomic motion [20,21]. The experimental scattering function $S_{exp}(Q, \omega)$ is fitted with the model incoherent scattering function,

$$S_{inc.}(Q,\omega) = A_0(Q)\delta(\omega) + A_1(Q)L(\omega,\Gamma) \quad (1)$$

convoluted with $R(Q, \omega)$. Here, $\delta(\omega)$ is the elastic δ-function, $L(\omega, \Gamma)$ is the Lorentzian function with the half-width Γ, and $A_0 + A_1 = 1$. As an example of the data, Fig. 3 shows the QENS spectrum of $YFe_2H_{2.6}$ recorded at $T = 360$ K, $\lambda = 2.75$ Å, and $Q = 3.94$ Å^{-1}.

The Q dependence of the elastic incoherent structure factor (EISF) A_0 is related to the geometry of the localized H motion [20,21]. At a given temperature, we have simultaneously fitted the spectra for all Q with Eq. (1), assuming a common value of the quasielastic half-width Γ. This procedure yields the values of $A_0(Q)$ and Γ. The $A_0(Q)$ values have been further corrected for a small contribution of the host-metal nuclei to the elastic line. The Q dependences of the resulting EISF at three temperatures are shown in Fig. 4. As can be seen from this figure, at a given temperature, there is a reasonable agreement between the results obtained using different incident neutron wavelengths. The measured EISF appears to be temperature-dependent, decreasing with increasing T. Such a temperature dependence of the EISF was also observed for other Laves-phase hydrides [5,6,8,22–24], other intermetallic hydrides [25–27] and for solid solutions of hydrogen in rare-earth metals [28]. This feature suggests that only a fraction p of the H atoms participates in the fast localized motion, and this fraction increases with temperature. The fraction $1 - p$ of 'trapped' H atoms (at the frequency scale of our QENS measurements) can originate from host-lattice defects (such as local lattice distortions [19] discussed above) and/or from H–H interactions leading to formation of some short-range ordered H configurations at low temperatures [5,6,22]. With increasing temperature, such 'trapped' H configurations should be progressively destroyed by thermal fluctuations; this results in the increase in the 'mobile' fraction p.

As noted in the Introduction, hydrogen atoms in $YFe_2H_{2.6}$ partially occupy the sublattice of g sites with the positional parameters $x_g = 0.339$ and $z_g = 0.141$ [2]. The structure of this g-site sublattice (see Fig. 1) suggests two possible types of localized H motion. The first possibility is that a hydrogen atom jumps over six g sites forming a regular hexagon with the nearest-neighbor g–g distance $r_1 = 1.50$ Å. This type of localized H motion was observed in many cubic Laves-phase hydrides [5,6,23,29]. The second

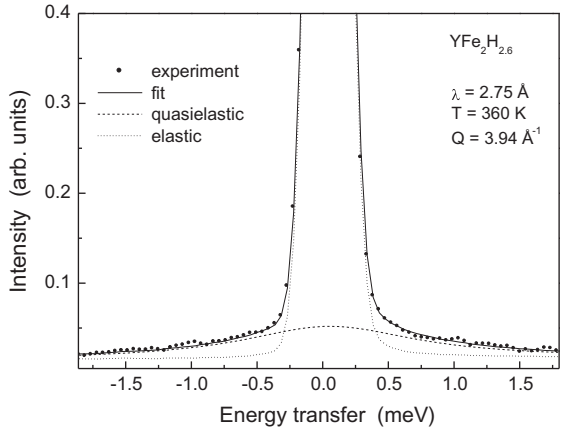

Fig. 3. The QENS spectrum for $YFe_2H_{2.6}$ measured on DCS at $\lambda = 2.75$ Å, $T = 360$ K and $Q = 3.94$ Å^{-1}. The full curve shows the fit of the two-component model (Eq. (1)) to the data. The dotted line represents the elastic component (the spectrometer resolution function), and the dashed line shows the Lorentzian quasielastic component.

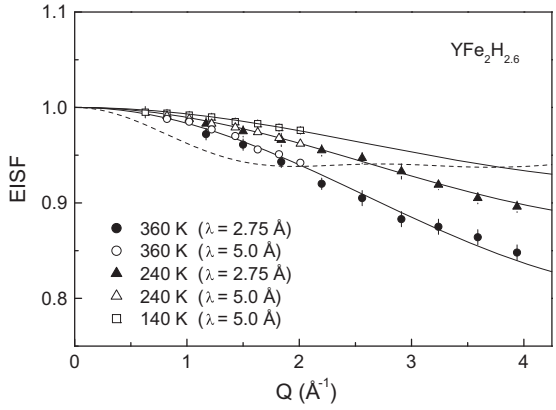

Fig. 4. The elastic incoherent structure factor for $YFe_2H_{2.6}$ measured at $T = 140$, 240 and 360 K. The solid curves show the fits of the two-site model (Eq. (3)) with the fixed $r_2 = 0.79$ Å to the data. The dashed curve shows the behavior of the EISF predicted by the six-site model (Eq. (2)) with the fixed $r_1 = 1.50$ Å.

possibility corresponds to back-and-forth jumps between two sites separated by $r_2 = 0.79$ Å. For the six-site model, the orientationally-averaged form of the EISF [20] is expressed as

$$\mathrm{EISF} = 1 - p + \frac{p}{6}\left[1 + 2j_0(Qr_1) + 2j_0(Qr_1\sqrt{3}) + j_0(2Qr_1)\right], \quad (2)$$

where $j_0(x) = \sin x/x$ is the spherical Bessel function of zeroth order. For the two-site model, the Q dependence of the orientationally-averaged EISF [20] is given by

$$\mathrm{EISF} = 1 - p + \frac{p}{2}[1 + j_0(Qr_2)] \quad (3)$$

It should be noted that the period of the oscillatory Q dependence of the EISF described by Eqs. (2) and (3) is determined by the corresponding distances between the sites (r_1 or r_2), while the value of p is responsible only for the amplitude of these oscillations. Comparison of the experimental Q dependences of the EISF with the models defined by Eqs. (2) and (3) shows that only the two-site model is consistent with the data. The solid lines in Fig. 4 represent the fits of the two-site model (Eq. (3)) with the fixed $r_2 = 0.79$ Å to the EISF data for $YFe_2H_{2.6}$ at three temperatures. It can be seen that Eq. (3) with p as the only fit parameter satisfactorily describes the observed Q dependence of the EISF at different temperatures. For comparison, the dashed line in Fig. 4 shows the behavior predicted by the six-site model (Eq. (2)) with the fixed $r_1 = 1.50$ Å. The six-site model predicts the EISF minimum near $Q = 2$ Å^{-1} and an increase in the EISF with increasing Q in the range 2.0–2.8 Å^{-1}, whereas the experimental EISF *decreases* in this range. Thus, the six-site model is inconsistent with the observed Q dependence of the EISF.

The temperature dependence of the rate τ_l^{-1} of localized H jumps, as derived from our QENS data for $YFe_2H_{2.6}$, is shown in Fig. 5. The half-width Γ of the quasielastic component obtained from the fits of QENS spectra to Eq. (1) is proportional to τ_l^{-1}; however, the exact relation between Γ and τ_l^{-1} depends on the model of localized motion [20]. For the two-site motion, $\Gamma = 2\hbar\tau_l^{-1}$ [20], and this relation has been used in our case. It can be seen from Fig. 5 that the temperature dependence of τ_l^{-1} in $YFe_2H_{2.6}$ deviates from the Arrhenius behavior. A similar feature was found for the temperature dependence of the localized H jump rate in a number of other Laves-phase hydrides [8,18,23,24,30]. Trying to fit the $\tau_l^{-1}(T)$ dependence for $YFe_2H_{2.6}$ by the Arrhenius law in different temperature ranges, we have obtained the activation energies of 42 and 10 meV in the ranges of 295–390 K and 140–240 K, respectively. The corresponding partial Arrhenius fits are shown by the dashed lines in Fig. 5. It should be noted that the observed change in the apparent activation energy cannot be attributed to any

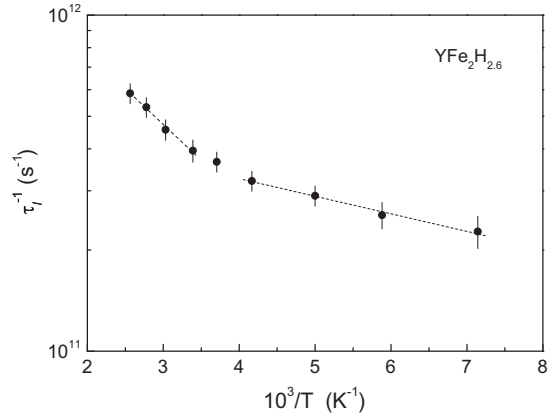

Fig. 5. The hydrogen jump rate derived from the width of the quasielastic component as a function of the inverse temperature. The dashed lines show the Arrhenius fits to the data in the ranges 295–390 K and 140–240 K.

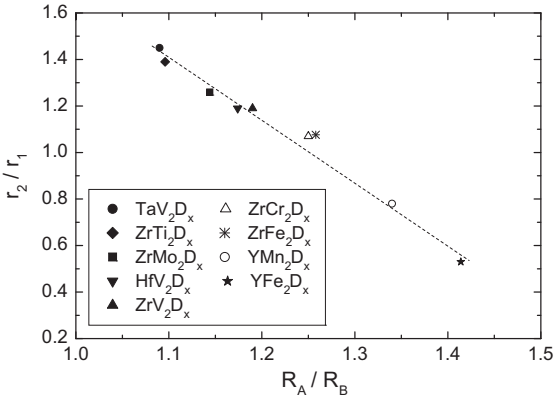

Fig. 7. The ratio of the g–g distances as a function of the ratio of metallic radii R_A/R_B for a number of C15-type deuterides AB_2D_x. The dashed line is a guide for an eye.

phase change in $YFe_2H_{2.6}$. In fact, in the course of our experiments on the time-of-flight neutron spectrometer DCS, the diffraction pattern of $YFe_2H_{2.6}$ has also been recorded, and we have not found any new Bragg peaks while cooling the sample from 390 K to 30 K. Most probably, the change in the apparent activation energy is related to the change in the mechanism of elementary H jumps, as in the case of hydrogen diffusion in b.c.c. metals [31].

In contrast to the case of YMn_2H_x [7], the slower type of H motion leading to long-range diffusion has not been observed for $YFe_2H_{2.6}$ in the studied temperature range. This motion remains too slow to contribute to the broadening of QENS spectra at the frequency scale of our measurements. It is likely that this feature originates from the peculiar g-site sublattice in $YFe_2H_{2.6}$ consisting of closely-spaced pairs (short r_2) well separated from each other (long r_1).

The temperature dependence of the fraction p, as derived from the fits of the EISF to the two-site model (Eq. (3)), is shown in Fig. 6. The fraction of H atoms participating in the fast localized motion increases nearly linearly with increasing temperature. Similar behavior of $p(T)$ was observed in a number of Laves phase hydrides [5,18,22]. The usual approach to the description of $p(T)$ is based on the assumption of a certain energy gap ΔE between 'trapped' and 'mobile' H states [28]. In the framework of this approach, a nearly linear temperature dependence of p suggests the presence of a broad distribution of ΔE values [5]. It should be noted that the values of p found for $YFe_2H_{2.6}$ are smaller than those for the other

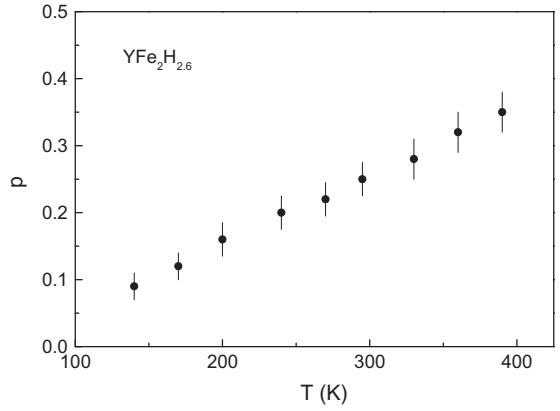

Fig. 6. The temperature dependence of the fraction of H atoms participating in the fast localized motion as derived from the fit of the two-site model (Eq. (3)) to the data for $YFe_2H_{2.6}$.

Laves phase hydrides in the same temperature ranges. This feature is consistent with considerable lattice distortions resulting from hydrogenation of YFe_2 [19].

In order to discuss a correlation between r_2/r_1 and the ratio of the metallic radii R_A/R_B for different cubic Laves phase hydrides, we have analyzed the available neutron diffraction data for C15-type deuterides AB_2D_x in which D atoms occupy interstitial g sites. The dependence of the positional parameters x_g and z_g on deuterium concentration in the same AB_2D_x compound is usually very weak. In the cases where neutron diffraction data are available for different deuterium concentrations x, we have used the positional parameters corresponding to lower x. The results are presented in Fig. 7 showing r_2/r_1 as a function of R_A/R_B for different cubic Laves phase deuterides. The values of r_2/r_1 have been derived from the neutron diffraction data for TaV_2D_x [32], $ZrTi_2D_x$ [33], $ZrMo_2D_x$ [34], HfV_2D_x [35], ZrV_2D_x [36], $ZrFe_2D_x$ [37], $ZrCr_2D_x$ [38], YMn_2D_x [39], and YFe_2D_x [2]. As can be seen from Fig. 7, the ratio r_2/r_1 (and thus, the structure of the g-site sublattice partially occupied by hydrogen) shows significant variations from one cubic Laves phase compound to another. With increasing R_A/R_B, the ratio r_1/r_2 tends to decrease. The point for YFe_2D_x with the smallest r_1/r_2 appears to be consistent with the nearly linear correlation between R_A/R_B and r_1/r_2. It should be noted that such a correlation may be used to predict general features of the microscopic picture of hydrogen jump motion in other cubic Laves phase hydrides where H dynamics has not yet been investigated.

4. Conclusions

The analysis of our quasielastic neutron scattering data for C15-type $YFe_2H_{2.6}$ has shown that the fast motional process in this system corresponds to localized jumps of H atoms within pairs of closely spaced interstitial g sites. In the studied T range of 140–390 K, the temperature dependence of the hydrogen jump rate τ_l^{-1} of this localized motion strongly deviates from the Arrhenius behavior; however, it can be reasonably described by two Arrhenius-like terms with the activation energies of 42 meV (in the range 295–390 K) and 10 meV (in the range of 140–240 K). The slower type of H motion leading to long-range diffusion has not been observed for $YFe_2H_{2.6}$ in the studied temperature range. This motion remains too slow to contribute to the broadening of QENS spectra at the frequency scale of our measurements. Hydrogen dynamics in $YFe_2H_{2.6}$ appears to be affected by considerable local lattice distortions resulting from hydrogenation of YFe_2. This is consistent with the large width of the H vibrational peaks in the inelastic neutron scattering spectrum and with the relatively small

fraction of H atoms participating in the fast localized jumps in $YFe_2H_{2.6}$.

Acknowledgments

This work utilized facilities supported in part by the National Science Foundation under Agreement no. DMR-0944772. This work was also supported by the Priority Program 12-P-2-1050 'Physico-technical principles of development of technologies and devices for smart adaptive electrical networks' of the Russian Academy of Sciences. A.V.S acknowledges financial support from the NIST Center for Neutron Research.

References

[1] G. Wiesinger, G. Hilscher, in: L. Schlapbach (Ed.), Hydrogen in Intermetallic Compounds I, Springer, Berlin, 1988, p. 285.
[2] V. Paul-Boncour, L. Guénée, M. Latroche, A. Percheron-Guégan, B. Ouladdiaf, F. Bourée-Vigneron, J. Solid State Chem. 142 (1999) 120.
[3] V. Paul-Boncour, S.M. Filipek, A. Percheron-Guégan, I. Marchuk, J. Pielaszek, J. Alloys Comp. 317–318 (2001) 83.
[4] V. Paul-Boncour, A. Percheron-Guégan, J. Alloys Comp. 293–295 (1999) 237.
[5] A.V. Skripov, J.C. Cook, D.S. Sibirtsev, C. Karmonik, R. Hempelmann, J. Phys.: Condens. Matter 10 (1998) 1787.
[6] A.V. Skripov, Defect Diffus. Forum 224–225 (2003) 75.
[7] A.V. Skripov, J.C. Cook, T.J. Udovic, M.A. Gonzalez, R. Hempelmann, V.N. Kozhanov, J. Phys.: Condens. Matter 15 (2003) 3555.
[8] A.V. Skripov, M.A. Gonzalez, R. Hempelmann, J. Phys.: Condens. Matter 18 (2006) 7249.
[9] V. Paul-Boncour, L. Guénée, M. Latroche, A. Percheron-Guégan, J. Alloys Comp. 255 (1997) 195.
[10] T. Leblond, V. Paul-Boncour, A. Percheron-Guégan, J. Alloys Comp. 446–447 (2007) 419.
[11] T.J. Udovic, C.M. Brown, J. Leão, P.C. Brand, R.D. Jiggetts, R. Zeitoun, T.A. Pierce, I. Peral, J.R.D. Copley, Q. Huang, D.A. Neumann, R.J. Fields, Nucl. Instrum. Methods A 588 (2008) 406.
[12] J.R.D. Copley, J.C. Cook, Chem. Phys. 292 (2003) 477.
[13] D. Richter, R. Hempelmann, R.C. Bowman, in: L. Schlapbach (Ed.), Hydrogen in Intermetallic Compounds II, Springer, Berlin, 1992, p. 97.
[14] D.K. Ross, in: H. Wipf (Ed.), Hydrogen in Metals III, Springer, Berlin, 1997, p. 153.
[15] M. Kemali, C.E. Buckley, D.K. Ross, S.M. Bennington, S.F. Parker, Physica B 234–236 (1997) 906.
[16] J.F. Fernandez, M. Kemali, D.K. Ross, S. Sanchez, J. Phys.: Condens. Matter 11 (1999) 10353.
[17] A.V. Skripov, H. Natter, R. Hempelmann, Solid State Commun. 120 (2001) 265.
[18] A.V. Skripov, T.J. Udovic, J.J. Rush, M.A. Uimin, J. Phys.: Condens. Matter 23 (2011) 065402.
[19] V. Paul-Boncour, G. Wiesinger, C. Reichl, M. Latroche, A. Percheron-Guégan, R. Cortes, Physica B 307 (2001) 277.
[20] M. Bée, Quasielastic Neutron Scattering, Hilger, Bristol, 1988.
[21] R. Hempelmann, Quasielastic Neutron Scattering and Solid State Diffusion, Clarendon, Oxford, 2000.
[22] A.V. Skripov, M. Pionke, O. Randl, R. Hempelmann, J. Phys.: Condens. Matter 11 (1999) 1489.
[23] A.V. Skripov, J.C. Cook, T.J. Udovic, V.N. Kozhanov, Phys. Rev. B 62 (2000) 14099.
[24] A.V. Skripov, T.J. Udovic, J.J. Rush, Phys. Rev. B 76 (2007) 104305.
[25] E. Mamontov, T.J. Udovic, O. Isnard, J.J. Rush, Phys. Rev. B 70 (2004) 214305.
[26] R.L. Cappelletti, Z. Chowdhuri, T.J. Udovic, R.M. Dimeo, B.C. Hauback, A.J. Maeland, Phys. Rev. B 73 (2006) 224109.
[27] A.V. Skripov, N.V. Mushnikov, P.B. Terent'ev, V.S. Gaviko, T.J. Udovic, J.J. Rush, J. Phys.: Condens. Matter 23 (2011) 405402.
[28] N.F. Berk, J.J. Rush, T.J. Udovic, I.S. Anderson, J. Less-Common Met. 172–174 (1991) 496.
[29] D.J. Bull, D.P. Broom, D.K. Ross, Chem. Phys. 292 (2003) 253.
[30] A.V. Skripov, M.A. Gonzalez, R. Hempelmann, J. Phys.: Condens. Matter 20 (2008) 085213.
[31] M. Hampele, G. Majer, R. Messer, A. Seeger, J. Less-Common Met. 172–174 (1991) 631.
[32] P. Fischer, F. Fauth, A.V. Skripov, A.A. Podlesnyak, L.N. Padurets, A.L. Shilov, B. Ouladdiaf, J. Alloys Comp. 253–254 (1997) 282.
[33] A.V. Skripov, T.J. Udovic, Q. Huang, J.C. Cook, V.N. Kozhanov, J. Alloys Comp. 311 (2000) 234.
[34] P. Fischer, F. Fauth, A.V. Skripov, V.N. Kozhanov, unpublished results.
[35] A.V. Irodova, V.P. Glazkov, V.A. Somenkov, S.Sh. Shil'shtein, Sov. Phys. Solid State 22 (1980) 45.
[36] J.J. Didisheim, K. Yvon, D. Shaltiel, P. Fischer, P. Bujard, E. Walker, Solid State Commun. 32 (1979) 1087.
[37] V. Paul-Boncour, F. Bourée-Vigneron, S.M. Filipek, I. Marchuk, I. Jacob, A. Percheron-Guégan, J. Alloys Comp. 356–357 (2003) 69.
[38] H. Kohlmann, F. Fauth, P. Fischer, A.V. Skripov, V.N. Kozhanov, K. Yvon, J. Alloys Comp. 327 (2001) L4.
[39] M. Latroche, V. Paul-Boncour, J. Przewoznik, A. Percheron-Guégan, F. Bourée-Vigneron, J. Alloys Comp. 231 (1995) 99.